applied optics

Measuring spatiotemporal ultrafast field structures of pulses from multimode optical fibers

ZHE GUANG,* MICHELLE RHODES, AND RICK TREBINO

School of Physics, Georgia Institute of Technology, 837 State Street, Atlanta, Georgia 30332, USA
**Corresponding author: zguang3@gatech.edu*

Received 4 January 2017; revised 20 March 2017; accepted 20 March 2017; posted 22 March 2017 (Doc. ID 283874); published 13 April 2017

Ultrashort pulses emerging from multimode optical fibers are spatiotemporally complex, because inside these fibers the modes have different spatial intensity patterns and experience different propagation velocities and dispersions. To determine the spatiotemporal field from multimode fibers, we applied a technique for the complete measurement of the output pulses called a spatially and temporally resolved intensity and phase evaluation device: full information from a single hologram. It yields the complete electric field over space and time from multiple digital holograms, simultaneously recorded at different frequencies on a single camera frame. Using femtosecond pulses from a Ti:sapphire laser, we measured the first few linearly polarized modes (LP_{01}, LP_{11}, LP_{02}, and LP_{21}) inside several few-mode fibers. We also generate movies displaying the measured spatial, temporal, and spectral field features.

OCIS codes: (320.0320) Ultrafast optics; (320.7100) Ultrafast measurements; (060.2310) Fiber optics; (090.1995) Digital holography.

https://doi.org/10.1364/AO.56.003319

1. INTRODUCTION

Multimode fiber (MMF) is now receiving increasing attention. This is partly because MMF can play an important role in expanding the transmission volume in optical telecommunications. With their larger core areas, MMFs allow mode-division multiplexing and hence a significant increase in the number of available data channels [1]. Data transmission using the first few linearly polarized (LP) modes has also been reported [2]. Terabit-scale transmission has also been achieved using modes that conserve orbital angular momentum both in free space [3] and in optical fibers [4]. In addition, using MMF mode interference, numerous sensors have been developed to measure refractive index, temperature, microdisplacement, and other important quantities, and are quite attractive due to their high sensitivity, and easy yet inexpensive fabrication [5]. Also, MMFs have been used in waveform control [6,7], microendoscopic imaging [8], and biophotonics manipulation [9]. For intense pulses, the large core areas of MMFs provide high damage thresholds for applications such as fiber-laser amplification [10], intense pulse delivery [11], and generating nonlinear optical effects (such as supercontinuum generation) [12].

Essentially all applications of MMFs depend on the information of the optical fields, including quantities such as the total power, chromatic dispersion, spatial mode pattern, and mode dispersion. Due to the different spatial and temporal behaviors of various MMF modes, the output fiber fields are in general spatiotemporally complex, especially when ultrashort pulses are involved; the various modes can merge in time and spread in length by differing amounts due to mode-dependent dispersions, as in Fig. 1.

Characterization of such complex ultrashort pulses in general has never been a trivial task. Modern ultrafast laser pulses contain temporal variations faster than the detectable limit of electronics, so they can be characterized only in detail by nonlinear optical approaches. Frequency-resolved optical gating (FROG) [13] is a well-known measurement method, yielding a pulse temporal intensity and phase measurement. Many various designs of FROG have been demonstrated over the years for different pulse durations and wavelengths. Unfortunately, FROG requires pulses to be smooth in spatial variations, and it only yields the pulse temporal profile. A simple, single-shot version of FROG, named GRENOUILLE [14], can characterize a few first-order spatiotemporal distortions in addition [15,16]. Pulses emerging from MMFs, however, can usually be more complex in space and time. To understand ultrashort pulse propagation in MMFs, it is helpful to perform the complete measurement to yield the field intensity and phase over time and space simultaneously.

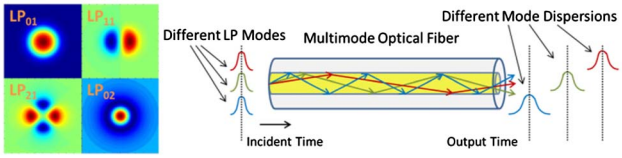

Fig. 1. Spatial, temporal, and spectral pulse field structures, due to multiple LP modes in propagation in MMFs.

Numerous characterization methods have been demonstrated to measure MMF output signals. They include spatially and spectrally resolved (S^2) imaging [17], cross-correlation (C^2) imaging [18], fast camera measurement [12], and time-gated spatial heterodyne interferometry [19]. These methods can extract very useful information regarding the measured optical field, such as the multipath interference [17]. However, they require scanning over space, wavelength, or time to capture the field information, which sets requirements on the laser source stability, optomechanical accuracy, and the pulse time needed to perform the measurement. Also, these methods usually require assumptions on the modal fields in order to reconstruct the full spatiotemporal field. Other methods, such as computer-generated holographic correlation filtering [20] and mode-decomposition analysis based on field intensity profile [21], have also been proposed for optical fiber field measurements. However, they can be complex in setup or computation, require stable modal contents among modes, and measure only a certain set of modes known to be present. A quick and complete method for measuring MMF pulses would therefore be beneficial.

2. METHOD

To measure the complete spatiotemporal intensity and phase, we have developed a pulse characterization technique called spatially and temporally resolved intensity and phase evaluation device: full information from a single hologram (STRIPED FISH) [22–24]. STRIPED FISH requires a spatially filtered reference pulse to be measured first by a FROG. Then, STRIPED FISH generates multiple holograms by crossing the unknown pulse beam with the reference pulse beam at different frequencies, with all holograms recorded by a single camera frame. This device only needs a single camera frame and thus no scanning, and by retrieving the holograms, it measures the unknown pulse field $E(x, y, t)$ over space and time (the field z dependence can be determined by performing diffraction integrals). In this work, we use STRIPED FISH to measure pulses from several few-mode fibers. In each measurement, we analyzed the STRIPED FISH trace, retrieved the pulse field, and plotted the pulse movie based on measured data to display the mode field spatial, temporal, and spectral variations.

STRIPED FISH apparatus is shown in Fig. 2. It comprises (1) a two-dimensional coarse grating as a diffractive optical element (DOE), fabricated by photomasking a quartz plate with chrome opaque coatings; (2) an interference bandpass filter (IBPF) to spectrally resolve the pulse; (3) associated imaging optics to image the holograms onto the camera frame with minimal aberrations; and (4) a camera to record multiple holograms [23]. Specifically, STRIPED FISH crosses the unknown and reference beams at a vertical angle at the DOE. The

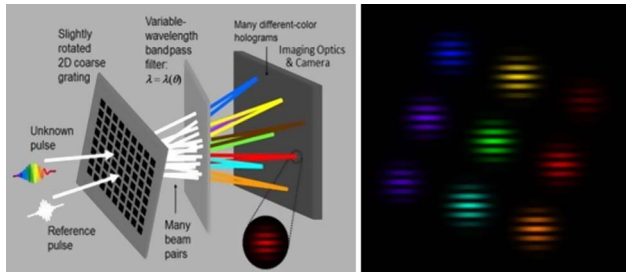

Fig. 2. Conceptual schematic of STRIPED FISH apparatus (left), showing only the key optical components. A spatiotemporally known reference pulse (spatially filtered and measured in time by FROG) and a potentially complex, unknown pulse are interfered on a camera, generating a tilted array of multiple digital holograms, each at a different frequency (right).

DOE diffracts both beams into multiple orders in both horizontal and vertical directions. We also slightly rotate the DOE in order to generate a tilted hologram array, so that the resulting pairs of diffracted beams propagate at different horizontal angles relative to the IBPF. The IBPF then spectrally filters out the beams, with the passband depending on the beam incidence angle. We also use an apodizing neutral density filter (ANDF), which is an element with a radially decreasing optical attenuation to compensate the diffraction efficiency imposed by the DOE to multiple diffractive orders. A pair of photographic lenses are also applied to reduce the optical aberrations related to the off-axis beam propagations. As a result, each beam pair transmits through the IBPF at a different wavelength and forms a hologram on the camera. Each digital hologram then contains the information required to compute the spatial intensity and phase at that particular wavelength. The recorded multiple holograms form the STRIPED FISH trace [25], which is sufficient to determine the unknown pulse complete spatiotemporal intensity and phase using a Fourier synthesis algorithm. We have previously demonstrated STRIPED FISH to measure complex pulses [23]. For MMF output pulses, we apply our STRIPED FISH apparatus to measure the spatiotemporal modal field, which determines the pulse arrival time, dispersions, and spatial field patterns of various modes emerging from the fiber.

After retrieving the spatiotemporal electric field $E(x, y, t)$ of a pulse, the multidimensional $E(x, y, t)$ quantity contains much information that is difficult to be plotted in a conventional manner. Two-dimensional plots of $E(x, t)$ or $E(y, t)$, such as such those in Ref. [22], are appropriate to show the pulse-field information when there is cylindrical symmetry or when only one-dimensional pulse information is of interest. The multidimensional complex field that we obtain from STRIPED FISH requires dynamic three-dimensional pulse-field plots demonstrating both intensity and phase information over two spatial dimensions and one temporal dimension at the measurement plane. To present the information intuitively as the human eye would see it, supposing its response time were fast enough to resolve ultrashort pulses, we use a spectrogram-based plotting method: the measured spatiotemporal unknown field $E(x, y, t)$ is gated by a numerical Gaussian temporal gate $g(t - \tau)$, yielding spectrograms at each space-time voxel:

$$Sp(x, y, \omega, \tau) = \left| \int_{-\infty}^{\infty} E(x, y, t) g(t - \tau) \exp(-i\omega t) \mathrm{d}t \right|^2.$$

The collection of spectrograms $Sp(x, y, \omega, \tau)$ represents the spectral energy distribution of the pulse for the spatial coordinates (x, y) in each gated local temporal segment at τ. We then color-code these spectrograms into delay-dependent color intensity distributions by calculating overlap integrals with spectral response functions, in which the long, middle, and short wavelengths of the pulse spectrum are represented by red, green, and blue colors. Specifically, they are

$$R(x, y, \tau) = \int_{-\infty}^{\infty} Sp(x, y, \omega, \tau) R(\omega) \mathrm{d}\omega,$$

$$G(x, y, \tau) = \int_{-\infty}^{\infty} Sp(x, y, \omega, \tau) G(\omega) \mathrm{d}\omega,$$

$$B(x, y, \tau) = \int_{-\infty}^{\infty} Sp(x, y, \omega, \tau) B(\omega) \mathrm{d}\omega.$$

The R, G, and B functions are all spectral response functions, defined based on the overall span of the pulse spectrum. In this work, the $R(\omega)$ is a Gaussian function centered at 2.29 rad/fs (823 nm); $G(\omega)$ is a Gaussian function centered at 2.36 rad/fs (800 nm); $B(\omega)$ is a Gaussian function centered at 2.42 rad/fs (777 nm). Their RMS widths are all 0.0316 rad/fs. From these color distributions, we plot a movie as a function of x, y, and τ to display all the information.

3. EXPERIMENT

Our experimental setup for MMF output-pulse measurement is shown in Fig. 3. Pulses from a Ti:sapphire laser (about 60 fs in duration, 23 nm FWHM) centered at 800 nm were sent through a spatial filter consisting of two lenses (of focal lengths 200 mm and 100 mm) and a pinhole (75 μm in diameter). When the flip mirror (FM) was in the beam, the spatially filtered pulse was characterized by a FROG device (Swamp Optics, GRENOUILLE, model 8-50). When the FM was out of beam, a beam splitter (BS) reflected part of the pulse energy (∼10%) to serve as the reference pulse, which was then synchronized by a translation stage to interfere with the unknown pulse. The remaining majority of the pulse energy passed through a single-prism pulse compressor (Swamp Optics, BOA) [26], which introduced negative chirp to the pulse before it entered the MMF in order to yield short output pulses. Dispersion compensation makes it easier to separate and identify the different LP pulse modes. Pulses were sent into and out of MMFs using objective lenses (Newport M – 60X; Japan 20 × 0.40), with fiber alignment adjusted by a homemade 6-axis fiber mount. The power coupled into fibers was on the order of 10 mw (up to 50 mw), with a ∼100 MHz pulse repetition rate. Due to the low pulse energy and low optical nonlinearity of the used fibers, the pulses were propagated in a linear regime. Small changes in the fiber alignment by as little as several microns in displacement can significantly influence the laser coupling efficiency into various modes. For example, on- and off-axis alignments of a dual-mode fiber SMF980 are shown in the insets of Fig. 3. After the MMF, the beam was collimated and combined with the reference pulse by another BS into the STRIPED FISH device.

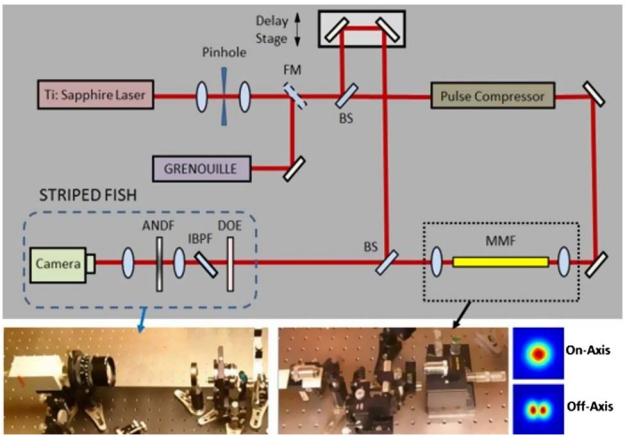

Fig. 3. Apparatus for self-referenced measurement setup to measure pulses from MMFs. A spatial filter made of two lenses and a pinhole, and a FROG device (GRENOUILLE) yield a spatiotemporally smooth reference pulse. A pulse compressor introduces negative chirp to precompensate fiber dispersion for better mode separation and discrimination. Adjusting the alignment of fiber coupling optics can control the energy coupled into each mode. The STRIPED FISH device is shown in the bottom-left figure. The bottom-middle figure is a picture of the fiber coupling stage with two coupling objective lenses. The inset in the figure on the bottom-right shows the results for the cases of on-axis and off-axis alignments, and their intensities output from the SMF980 fiber.

For simplicity, we studied MMFs that support the first few LP modes under weakly guiding conditions. To study LP_{01} and LP_{11} modes, we used single-mode fibers designed for 980 nm (Thorlabs, 980 HP and SMF980-5.8-125, 238 mm and 235 mm lengths) to operate as dual-mode fibers for our pulses at 800 nm, as the fibers have larger core areas than 800 nm single-mode fibers. We also used 1550 nm single-mode fiber (Thorlabs, SMF28, 106 mm length) to study four modes in 800 nm pulses. The pulse compressor was adjusted to give negative group-delay dispersion ($-8500\ \mathrm{fs}^2 \sim -12000\ \mathrm{fs}^2$) to approximately compensate for the dispersion of the fundamental mode LP_{01} for each fiber. The exact amount of negative dispersion was determined by performing another FROG measurement after the MMF and output objective lens when the LP_{01} mode (close to Gaussian in space) was present and adjusting until the measured chirp was zero. Even though the signal pulses were generally longer in time than the reference pulse, they should be of the same spectral range due to the low pulse-induced nonlinearity, and interferometry would work to measure the signal pulse, as long as it interferes with the reference pulse.

4. RESULTS

Figures 4(a) and 4(c) show the STRIPED FISH traces of LP_{01} and LP_{11} modes, respectively, from the same fiber (SMF980, 235 mm length), generated by varying the fiber coupling conditions to preferentially excite each mode individually. When only the fundamental mode LP_{01} was present, the measured trace was similar to a trace of a Gaussian pulse [25]. When the secondary LP_{11} mode contained most of the energy, the STRIPED FISH holograms showed two intensity lobes with a fringe discontinuity between them, which reflects the phase

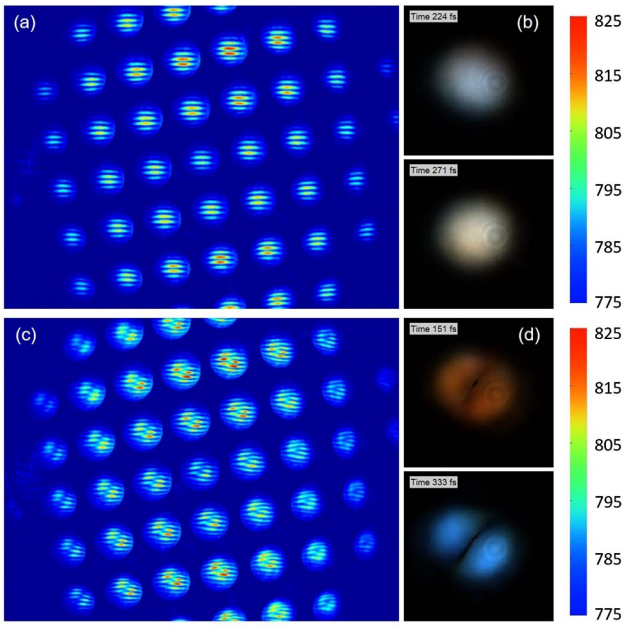

Fig. 4. (a) STRIPED FISH trace of LP_{01} mode from SMF980. (b) Retrieved pulse movie of LP_{01} mode (see Visualization 1). (c) STRIPED FISH trace of LP_{11} mode from SMF980. (d) Retrieved pulse movie of LP_{11} mode (see Visualization 2).

jump in the LP_{11} modal field. Two time snapshots from each measured pulse movie are displayed in Figs. 4(b) and 4(d). In each movie, the measured pulse propagates out of the screen, with brightness indicating intensity and color change denoting frequency variation over time. As expected, the pulse in the LP_{01} mode has a Gaussian shape and shows almost no color (frequency) variation over time, and the LP_{11} pulse shows a double-lobed intensity with color variation in time (spectral dispersion about 2.9×10^{-4} rad/fs^2) and a much longer pulse duration (about 250 fs).

We used another MMF at 800 nm (SMF28, 106 mm length) to study the behavior of four modes LP_{01}, LP_{11}, LP_{21}, and LP_{02} of pulses. As in Fig. 5, in this particular case, energy was coupled well into three LP modes (LP_{01}, LP_{21}, LP_{02}), and the LP_{11} mode had a low coupling efficiency and thus low visibility. The LP_{11} mode coupling could be increased by aligning the exciting pulse more in off-axis directions, although this resulted in less energy being coupled into other modes. We show the measured STRIPED FISH trace and snapshots of the retrieved pulse movie in Figs. 5(a) and 5(b). The measured trace differs from Fig. 4(a) of a Gaussian pulse, showing intensity patterns due to the mixture of different modes. The central part of each hologram is quite bright due to the LP_{01} mode, and the relatively dim peripheral parts show intensity beating distribution among other modes. In the movie, it is clear that three different fiber modes were present, with consecutive arrival time. Each mode is almost white in color, indicating little chirp in the modes. These pulse characteristics mean that the modes have different propagation velocities but very similar spectral dispersions. The coloring of the LP_{02} mode (4.5×10^{-5} rad/fs^2) observed in the movie visualization is likely caused by temporal interference with the trailing edge of the LP_{21} mode (1.1×10^{-4} rad/fs^2).

The first two fibers that we measured had differences in modal velocities that caused the modes to be well separated in time after the fiber. However, in practical cases, not all fibers have significant differences in modal velocities, and modes that may not be separable in time can be more difficult to measure. As STRIPED FISH measures the complete transverse complex electric field, it can characterize fiber modes that overlap in time as well. As in Fig. 6, we measured a pulse with simultaneously excited LP_{01} and LP_{11} modes from a two-mode fiber (980 HP, 238 mm length). In Fig. 6(a), the STRIPED FISH trace from this measurement shows an intermediate holographic pattern between those of LP_{01} and LP_{11}, indicating the presence of both modes in pulse. Specifically, hologram intensity is in a superposition form of LP_{01} mode and LP_{11} mode pattern, and hologram fringes vary more gradually across the middle than Fig. 4(c). In addition, lobes on the left and the right show intensity beating from hologram to hologram, which indicates spectral beating between the LP_{01} and LP_{11} modes. In Fig. 6(b), the pulse movie shows two temporally overlapping modes. The chirped LP_{11} mode (4.7×10^{-4} rad/fs^2) in the wings is significantly longer than the nonchirped LP_{01} mode, which only shows up briefly in the middle. Because these modes propagate at such similar velocities, they continue overlap in time, no matter how much length of fiber the pulse travels through. The velocities of different LP modes are dependent

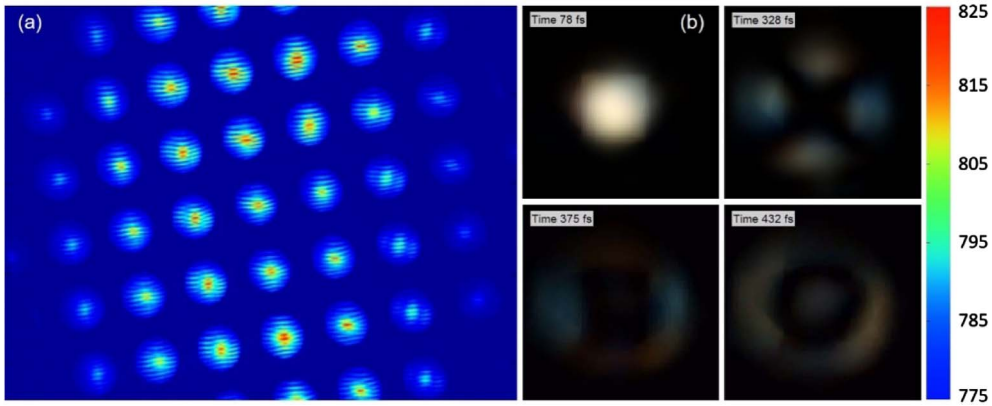

Fig. 5. (a) STRIPED FISH trace for a four-mode fiber SMF28. (b) Retrieved pulse movie (see Visualization 3).

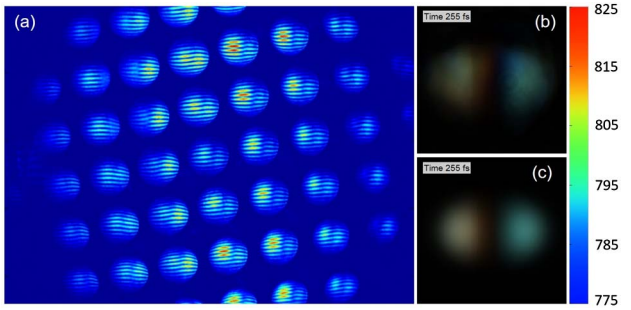

Fig. 6. (a) STRIPED FISH trace for mixing LP_{01} and LP_{11} modes from 980 HP. (b) Retrieved pulse movie of 980 HP (see Visualization 4). (c) Reconstructed movie using field decomposition approach of the STRIPED FISH measured field (see Visualization 5).

on fiber structure parameters and also the frequency in consideration, as studied in Ref. [27].

When modes cannot be separated over space and time, determining how much energy each mode accounts for in the field becomes more important and useful. From the measurement, STRIPED FISH yields the spatiotemporal electric field $E(x, y, t)$ or, equivalently, the spatiospectral field $E(x, y, \omega)$ by Fourier transform. LP fiber modes $E_{\mathrm{lp}}(x, y, \omega)$ form an orthogonal set, onto which an arbitrary field $E_{\mathrm{arb}}(x, y, \omega)$ can be decomposed by calculating overlap integrals. The resulting modal weight coefficient w_{lp} is

$$w_{\mathrm{lp}}(\omega) = \frac{\left|\iint E_{\mathrm{arb}} E_{\mathrm{lp}}^{*} \mathrm{d}x\mathrm{d}y\right|^2}{\iint |E_{\mathrm{arb}}|^2 \mathrm{d}x\mathrm{d}y \iint |E_{\mathrm{lp}}|^2 \mathrm{d}x\mathrm{d}y}.$$

These modal weight coefficients depend on frequency or, equivalently, on time. The weight coefficients $w_{\mathrm{lp}}(\omega)$ are essential to determine the modal content distribution of the pulse energy among the multiple allowable propagation modes of the fiber. Once this coefficient is determined for each mode, the relative mode intensities are determined up to a constant scaled by the total pulse energy. Then the phase information of the pulse modes, or relative arrival time of the modes, can be retrieved from the imaginary part of the inner product between the arbitrary field and the modal field. As an example, in the case of 980 HP [Figs. 6(a) and 6(b)], where the modes were inseparable in time, we determined the energy in LP_{01} and LP_{11} from the measured field and generated a reconstructed pulse movie by performing the calculation and used the field intensity and phase coefficients to reproduce a pulse movie [Fig. 6(c)]. The resulting movie is in good agreement with the measured movie in Fig. 6(b), with similar spatial intensity distribution and temporal frequency interference shown by the color variations. Mode content coefficients from excitation can be calculated using overlap integrals, when fiber modes overlap in time and space, which can be used to present modes in the pulse movie.

5. CONCLUSION

To conclude, STRIPED FISH offers a solution for measuring MMF pulse spatiotemporal fields. Using several fibers under different launching conditions, multiple spatiotemporal pulses were generated, measured, and displayed. Our current apparatus has a temporal range limited to a few hundred femtoseconds by the spectral pass bandwidth of the IBPF, so it can measure only a few MMF modes that are not much separated in time. To measure more modes with largely different modal propagation speeds, the characterization can be performed by using a narrower bandpass filter (<1 nm) or by introducing a coarse delay scan of the reference pulse to increase the temporal range (and reciprocally, the spectral resolution). In its existing state, STRIPED FISH can make measurements on few-mode fibers and display intuitively, and by performing overlap integrals, it is feasible to extract the measured field modal information. With fiber dispersion compensated, pulses in the first few LP modes were demonstrated with their different spatial intensity patterns, temporal velocities, and spectral dispersion properties.

Funding. National Science Foundation (NSF) (#ECCS-1307817, #ECCS-1609808); Georgia Research Alliance (GRA).

Acknowledgment. We thank Don Harter for suggesting this problem to us, and acknowledge John Buck, Fumin Zhang, and Tomthin Nganba Wangjam for their help and discussions.

REFERENCES

1. W. D. Mark, "Spectral analysis of the convolution and filtering of non-stationary stochastic processes," J. Sound Vib. **11**, 19–63 (1970).
2. R. Ryf, S. Randel, A. H. Gnauck, C. Bolle, A. Sierra, S. Mumtaz, M. Esmaeelpour, E. C. Burrows, R.-J. Essiambre, and P. J. Winzer, "Mode-division multiplexing over 96 km of few-mode fiber using coherent 6 6 MIMO processing," J. Lightwave Technol. **30**, 521–531 (2012).
3. P. Lissberger and W. Wilcock, "Properties of all-dielectric interference filters. II. Filters in parallel beams of light incident obliquely and in convergent beams," J. Opt. Soc. Am. **49**, 126–128 (1959).
4. M. Bass, E. W. Van Stryland, D. R. Williams, and W. L. Wolfe, *Handbook of Optics* (McGraw-Hill, 2001).
5. Q. Wu, Y. Semenova, P. Wang, and G. Farrell, "High sensitivity SMS fiber structure based refractometer-analysis and experiment," Opt. Express **19**, 7937–7944 (2011).
6. O. Katz, E. Small, Y. Bromberg, and Y. Silberberg, "Focusing and compression of ultrashort pulses through scattering media," Nat. Photonics **5**, 372–377 (2011).
7. E. E. Morales-Delgado, S. Farahi, I. N. Papadopoulos, D. Psaltis, and C. Moser, "Delivery of focused short pulses through a multimode fiber," Opt. Express **23**, 9109–9120 (2015).
8. I. N. Papadopoulos, S. Farahi, C. Moser, and D. Psaltis, "High-resolution, lensless endoscope based on digital scanning through a multimode optical fiber," Biomed. Opt. Express **4**, 260–270 (2013).
9. T. Čižmár and K. Dholakia, "Shaping the light transmission through a multimode optical fibre: complex transformation analysis and applications in biophotonics," Opt. Express **19**, 18871–18884 (2011).
10. D. Richardson, J. Nilsson, and W. Clarkson, "High power fiber lasers: current status and future perspectives [Invited]," J. Opt. Soc. Am. B **27**, B63–B92 (2010).
11. H. Itoh, T. Urakami, S.-I. Aoshima, and Y. Tsuchiya, "Femtosecond pulse delivery through long multimode fiber using adaptive pulse synthesis," Jpn. J. Appl. Phys. **45**, 5761–5763 (2006).
12. Y. Vidne and M. Rosenbluh, "Spatial modes in a PCF fiber generated continuum," Opt. Express **13**, 9721–9728 (2005).
13. R. Trebino, K. W. DeLong, D. N. Fittinghoff, J. N. Sweetser, M. A. Krumbügel, and D. J. Kane, "Measuring ultrashort laser pulses in the time-frequency domain using frequency-resolved optical gating," Rev. Sci. Instrum. **68**, 3277–3295 (1997).

14. P. O'shea, M. Kimmel, X. Gu, and R. Trebino, "Highly simplified device for ultrashort-pulse measurement," Opt. Lett. **26**, 932–934 (2001).
15. S. Akturk, M. Kimmel, P. O'shea, and R. Trebino, "Measuring spatial chirp in ultrashort pulses using single-shot frequency-resolved optical gating," Opt. Express **11**, 68–78 (2003).
16. S. Akturk, M. Kimmel, P. O'shea, and R. Trebino, "Measuring pulse-front tilt in ultrashort pulses using GRENOUILLE," Opt. Express **11**, 491–501 (2003).
17. J. Nicholson, A. Yablon, S. Ramachandran, and S. Ghalmi, "Spatially and spectrally resolved imaging of modal content in large-mode-area fibers," Opt. Express **16**, 7233–7243 (2008).
18. D. Schimpf, R. Barankov, and S. Ramachandran, "Cross-correlated (C^2) imaging of fiber and waveguide modes," Opt. Express **19**, 13008–13019 (2011).
19. R. Rokitski and S. Fainman, "Propagation of ultrashort pulses in multimode fiber in space and time," Opt. Express **11**, 1497–1502 (2003).
20. T. Kaiser, D. Flamm, S. Schröter, and M. Duparré, "Complete modal decomposition for optical fibers using CGH-based correlation filters," Opt. Express **17**, 9347–9356 (2009).
21. F. Stutzki, H.-J. Otto, F. Jansen, C. Gaida, C. Jauregui, J. Limpert, and A. Tünnermann, "High-speed modal decomposition of mode instabilities in high-power fiber lasers," Opt. Lett. **36**, 4572–4574 (2011).
22. P. Gabolde and R. Trebino, "Single-shot measurement of the full spatiotemporal field of ultrashort pulses with multispectral digital holography," Opt. Express **14**, 11460 (2006).
23. Z. Guang, M. Rhodes, M. Davis, and R. Trebino, "Complete characterization of a spatiotemporally complex pulse by an improved single-frame pulse-measurement technique," J. Opt. Soc. Am. B **31**, 2736–2743 (2014).
24. Z. Guang, M. Rhodes, and R. Trebino, "Measurement of the ultrafast lighthouse effect using a complete spatiotemporal pulse-characterization technique," J. Opt. Soc. Am. B **33**, 1955–1962 (2016).
25. Z. Guang, M. Rhodes, and R. Trebino, "Numerical simulations of holographic spatiospectral traces of spatiotemporally distorted ultrashort laser pulses," Appl. Opt. **54**, 6640–6651 (2015).
26. S. Akturk, X. Gu, M. Kimmel, and R. Trebino, "Extremely simple single-prism ultrashort-pulse compressor," Opt. Express **14**, 10101–10108 (2006).
27. D. Gloge, "Weakly guiding fibers," Appl. Opt. **10**, 2252–2258 (1971).